[13] Analysis of Reversibly Interacting Macromolecular Systems by Time Derivative Sedimentation Velocity

By WALTER F. STAFFORD

Sedimentation velocity boundary analysis of interacting systems can provide information about stoichiometries and equilibrium constants that is complementary to information obtained by equilibrium sedimentation analysis. The theoretical basis for the analysis of sedimentation boundaries was first developed in the 1950s by Gilbert and co-workers, who solved the transport equations of the case of no diffusion.[1–3] Extensive numerical simulations of the transport equations for various reversibly interacting systems were carried out by Cann,[4] Cox and Dale,[5] and others in the 1960s, 1970s, and 1980s and have given us a firm basis for the use of transport methods for the analysis of interacting systems.

This chapter discusses the application of time derivative techniques to the analysis of interacting systems by sedimentation velocity. Potential problems and limitations associated with the computation of weight average sedimentation coefficients for both rapidly reversible and kinetically limited systems in general are treated. An example of the application of finite element simulation software to the analysis of an antigen–antibody system at high dilution is given. A potential problem with convective instability of pressure-dependent systems is also discussed and shown not to be a problem if care is taken.

The accessible concentration range for sedimentation velocity has been extended considerably by the time derivative/signal averaging method.[6,7] The combination of taking the time derivative, which eliminates completely the time-independent optical background, and of averaging the time derivative curves results in a considerable increase in precision compared with older methods of analysis. Therefore, because of its sensitivity and selectivity, sedimentation velocity may be the only way the equilibrium constant for an interacting system can be estimated by sedimentation analysis. The

[1] G. A. Gilbert, *Proc. R. Soc.* **A250,** 377 (1959).
[2] G. A. Gilbert and R. C. Jenkins, *Proc. R. Soc.* **A253,** 420 (1959).
[3] G. A. Gilbert, *Discuss. Farad. Soc.* **20,** 68 (1955).
[4] J. R. Cann, "Interacting Macromolecules." Academic Press, New York, 1970.
[5] D. J. Cox and R. S. Dale, *in* "Protein–Protein Interactions" (C. Frieden, and L. W. Nichol, eds.), pp. 173–212. John Wiley & Sons, New York, 1981.
[6] W. F. Stafford, *Anal. Biochem.* **203,** 295 (1992).
[7] W. F. Stafford, *Methods Enzymol.* **240,** 478 (1994).

0076-6879/00 $30.00

increased sensitivity allows investigation of interacting systems that were previously inaccessible to ultracentrifugal analysis. Reversibly interacting systems whose dissociation constants in terms of mass concentration units are in the range of 5–100 μg/ml can be studied using Rayleigh optics, and those whose dissociation constants, expressed in optical density (OD) units, are less than 0.1 OD unit can be studied using UV optics.

Both kinetically controlled and pressure-dependent interacting systems may be difficult to analyze by sedimentation velocity. It is shown below that kinetically controlled systems can be treated to yield reliable association equilibrium constants from analysis of weight average sedimentation coefficients. Interactions whose reaction times are on the same order as the rates of sedimentation can be identified and treated. Furthermore, it is shown that the rate of reequilibration has little effect on the calculation of equilibrium constants from weight average sedimentation coefficients, as long as the system is at equilibrium at the start of sedimentation. Therefore, systems having both slow forward and slow reverse reaction rates can be studied by sedimentation velocity. This means that sedimentation velocity can be used to analyze some systems that might not be amenable to sedimentation equilibrium methods. For example, an interacting system that has a relaxation time on the order of 12 to 24 hr ($k_r = 5 \times 10^{-4}$ to 1×10^{-5} sec^{-1}, where k_r is the first-order dissociation rate constant) would require more than 10 days of sedimentation to analyze by sedimentation equilibrium but could be analyzed essentially as a quasistatic system by sedimentation velocity. Therefore, successful analysis is possible even when the system is reversible but not fast.

Sedimentation transport of pressure-dependent interacting systems can lead to the generation of negative concentration gradients.[8] In the absence of a stabilizing density gradient, convection can result. One might think that pressure effects would obviate the use of sedimentation velocity to study systems that exhibited any volume change on association because any volume change can in principle produce negative concentration gradients. However, it can be shown that for most interacting systems with even substantial volume changes that the stabilizing density gradient set up by redistribution of buffer components at the usual concentrations is expected to be enough to prevent convection as long as certain precautions are taken.

Two general approaches to the analysis of interacting systems are discussed. The first approach, which involves computing the weight average sedimentation coefficient as a function of concentration, is insensitive to details of boundary shape. The weight average sedimentation coefficient, s_w, is a composition-dependent parameter and, therefore, for any given

[8] G. Kegeles and W. F. Harrington, *Methods Enzymol.* **27,** 306 (1973).

system controlled by mass action, it will be a function of the plateau concentration only, reflecting the composition of the solution at the plateau concentration. Analysis of the functional dependence of s_w on plateau concentration allows the determination of the equilibrium constants describing the system. For some reviews of the analysis of interacting systems see the articles by Stafford,[9] Lee and Rajendran[10], and Rivas *et al.*[11] The weight average sedimentation coefficient has been used extensively by Timasheff and co-workers to study the self-association of tubulin under various conditions. For review of this work the reader is referred to articles by Na and Timasheff and to references contained therein.[12,13] The weight average sedimentation coefficient computed with the time derivative method[6,9] has been used extensively by Lobert, Correia, and co-workers[14–16] to study the effects of vinca alkaloids and nucleotides on the self-assembly of tubulin. Most recently, the weight average along with the Z and $Z + 1$ averages have been used by Toedt *et al.* to characterize a tobacco mosaic virus (TMV) coat protein mutant.[17]

The second general approach involves numerical solutions of the Lamm equation to simulate sedimentation boundary profiles for various values of the parameters describing the system. It can be subdivided further into two different methods. The first simulation method involves the generation of a series of sedimentation patterns spanning the suspected range of parameters followed by direct comparison with the observed patterns. This comparison approach was used extensively by Timasheff and co-workers[18–22] in the

[9] W. F. Stafford, *in* "Modern Analytical Ultracentrifugation: Acquisition and Interpretation of Data for Biological and Synthetic Polymer Systems" (T. M. Schuster and T. M. Laue, eds.), pp. 119–137. Birkhäuser, Boston, 1994.

[10] J. C. Lee and S. Rajendran, *in* "Modern Analytical Ultracentrifugation: Acquisition and Interpretation of Data for Biological and Synthetic Polymer Systems" (T. M. Schuster and T. M. Laue, eds.), pp. 138–155. Birkhäuser, Boston, 1994.

[11] G. Rivas, W. F. Stafford, and A. P. Minton, "Methods: A Companion to Methods in Enzymology," Vol. 19, pp. 194–212. Academic Press, San Diego, California, 1999.

[12] G. C. Na and S. N. Timasheff, *Methods Enzymol.* **117,** 496 (1985).

[13] G. C. Na and S. N. Timasheff, *Methods Enzymol.* **117,** 459 (1985).

[14] S. Lobert, B. Vulevic, and J. J. Correia, *Biochemistry* **35,** 6806 (1996).

[15] S. Lobert, C. A. Boyd, and J. Correia, *Biophys. J.* **72,** 416 (1997).

[16] S. Lobert, A. Frankfurter, and J. J. Correia, *Biochemistry* **34,** 8050 (1995).

[17] J. M. Toedt, E. H. Braswell, T. M. Schuster, D. A. Yphantis, Z. F. Taraporewala, and J. N. Culver, *Protein Sci.* **8,** 261 (1999).

[18] R. P. Frigon and S. N. Timasheff, *Biochemistry* **14,** 4567 (1975).

[19] R. P. Frigon and S. N. Timasheff, *Biochemistry* **14,** 4559 (1975).

[20] S. N. Timasheff, R. P. Frigon, and J. C. Lee, *Fed. Proc.* **35,** 1886 (1976).

[21] G. C. Na and S. N. Timasheff, *Biochemistry* **25,** 6214 (1986).

[22] G. C. Na and S. N. Timasheff, *Biochemistry* **25,** 6222 (1986).

1970s and 1980s, using schlieren optics in the 1-to 10-mg/ml range to analyze self-association of tubulin.

The second simulation method uses a nonlinear least-squares fitting procedure employing simulation software as a function evaluator. Unless the system can be parameterized in terms of a single dimensionless parameter, the nonlinear curve fitting approach is the better of these last two. Several examples of simulated single-parameter self-associating and heteroassociating systems have been discussed previously.[9] A description of global curve-fitting software for analyzing self-associating and heteroassociating interacting systems using numerical finite element solutions to the Lamm equation to fit to time difference data[23] will be described elsewhere. The first use of finite element simulations for curve fitting to sedimentation velocity data was originally presented by Todd and Haschemeyer.[24] The Todd–Haschemeyer method has been revived and reprogrammed by Demeler and Saber[25] and extended by Schuck,[26] using a moving reference frame to accelerate significantly the computations. More recently Schuck and Demeler[27] have developed a method for fitting for the time-invariant background component when using the Todd–Haschemeyer method for the analysis of both interference and absorbance data. These programs are available from the RASMB (Reversible Associations in Structural and Molecular Biology) FTP site (*ftp://rasmb.bbri.org/*) and can be used to analyze mixture of independently sedimenting species as well as monomer–dimer and monomer–trimer self-associations.

Sedimentation transport experiments are not carried out at thermodynamic equilibrium; therefore, care must be exercised to assure that equilibrium constants derived from weight average sedimentation coefficients actually reflect the equilibrium situation. There are several problems unique to sedimentation velocity analysis that need to be addressed in this regard; they include (1) the effects of radial dilution, which may cause a shift in the equilibrium during sedimentation, (2) hydrodynamic concentration dependence of the sedimentation coefficients for the species making up the system, (3) thermodynamic concentration dependence influencing the diffusion coefficients through the activity coefficient, (4) kinetics of reequilibration, and (5) negative concentration gradients resulting from pressure dependence of the equilibrium constants. The effects of hydrodynamic and thermodynamic nonideality can be minimized by performing experiments at sufficiently low concentration. They may cause significant problems in

[23] W. F. Stafford, *Biophys. J.* **74,** A301 (1998).
[24] G. P. Todd and R. H. Haschemeyer, *Proc. Natl. Acad. Sci. U.S.A.* **78,** 6739 (1981).
[25] B. Demeler and H. Saber, *Biophys. J.* **74,** 444 (1998).
[26] P. Schuck, *Biophys. J.* **75,** 1503 (1998).
[27] P. Schuck and B. Demeler, *Biophys. J.* **76,** 2288 (1999).

the analysis of weakly associating systems, which must be studied at concentrations higher than about 1 mg/ml if their effects are not taken into account. Their effects can be dealt with explicitly in curve-fitting routines and are not discussed further here. However, the other effects, which are addressed below, are relevant to all concentration ranges.

Background Theory for Time Derivative Method

The large increase in sensitivity of sedimentation analysis has been achieved mainly because of the development of on-line, real-time Rayleigh interferometric systems pioneered by Laue, Yphantis, *et al.*[28–31] These systems have been developed further and optimized for sedimentation velocity analysis.[7,9,31–33] The rapidity of on-line systems has allowed the convenient computation of the time derivative of the concentration distribution resulting in automatic baseline correction of the sedimentation patterns. Moreover, the ability to collect rapidly large amounts of data means the data can be effectively signal averaged to increase the signal-to-noise ratio.

A derivation of the apparent sedimentation coefficient distribution function, $g(s^*)$ versus s^*, from the time derivative has been presented previously.[6] It should be pointed out that the unnormalized apparent distribution function, designated as $g(s^*)$, can be considered as simply the first derivative of the concentration profile with respect to s^*, dc/ds^* versus s^*, and, therefore, contains all the contributions from diffusion. The original derivations of $g(s^*)$ both from the radial derivative[34,35] and from the time derivative[6] were based on the assumption that diffusion was negligible. It was recognized that the apparent distribution approached the "true" distribution either in the limit of high molecular weight (i.e., as D approached zero) or as the patterns were extrapolated to infinite time. In spite of these limitations and nomenclature, the uncorrected, unnormalized,

[28] T. M. Laue, Ph.D. dissertation. University of Connecticut, Storrs, Connecticut, 1981.
[29] M. S. Runge, T. M. Laue, D. A. Yphantis, M. R. Lifsics, A. Saito, M. Altin, K. Reinke, and R. C. Williams, Jr., *Proc. Natl. Acad. Sci. U.S.A.* **78,** 1431 (1981).
[30] D. A. Yphantis, *Biophys. J.* **45,** 324a (1984).
[31] D. A. Yphantis, J. W. Lary, W. F. Stafford, S. Liu, P. H. Olsen, D. B. Hayes, T. P. Moody, T. M. Ridgeway, D. A. Lyons, and T. M. Laue, *in* "Modern Analytical Ultracentrifugation: Acquisition and Interpretation of Data for Biological and Synthetic Polymer Systems" (T. M. Schuster and T. M. Laue, eds.), pp. 209–226. Birkhäuser, Boston, 1994.
[32] W. F. Stafford and S. Liu, *Prog. Biomed. Optics* **2386,** 130 (1995).
[33] W. F. Stafford, S. Liu, and P. E. Prevelige, *in* "Techniques in Protein Chemistry VI" (J. W. Crabb, ed.), pp. 427–432. Academic Press, San Diego, California, 1995.
[34] W. B. Bridgman, *J. Am. Chem. Soc.* **64,** 2349 (1942).
[35] H. Fujita, "Foundations of Ultracentrifugal Analysis." John Wiley & Sons, New York, 1976.

apparent distribution function, $\hat{g}(s^*)$, is a useful analytical tool. Because the $\hat{g}(s^*)$ versus s^* distribution is geometrically similar to the corresponding concentration gradient profile, dc/dr versus r, it contains all the same useful visual and analytical information.[9]

It is shown below that the assumption of no diffusion leads to an approximation in $\hat{g}(s^*)$ that must be taken into account only for low molecular weight materials (<50 kg/mol). Now we consider an exact derivation of $\hat{g}(s^*)$ and show how it is related to the original approximate derivation. The following derivation of dc/ds^* from the time derivative makes no assumptions about diffusion and, therefore, is completely general. The purpose of this derivation is twofold: (1) to present the complete derivation of the time derivative analysis and (2) to show the exact relation between the $\hat{g}(s^*)$ functions derived from the spatial derivative and from the time derivative, respectively.

Considering c as a function of s^* and t, $c = c\ (s^*, t)$, we can write

$$dc = \left(\frac{\partial c}{\partial t}\right)_{s^*} dt + \left(\frac{\partial c}{\partial s^*}\right)_t ds^* \tag{1}$$

where c is the concentration expressed on the c-scale and

$$s^* \equiv \frac{1}{\int_{t=0}^{t} \omega^2(t)dt} \ln\left(\frac{r}{r_m}\right)$$

where $\omega^2(t)$ is the angular velocity of the rotor as a function of time.

The factor in the denominator can be replaced by $\omega^2 t_{sed}$, where, t_{sed} is the effective time of sedimentation and ω is the final angular velocity of the rotor,

$$s^* \equiv \frac{1}{\omega^2 t_{sed}} \ln\left(\frac{r}{r_m}\right)$$

since

$$t_{sed} = \frac{\int_{t=0}^{t} \omega^2(t)dt}{\omega^2}$$

In all equations, t is meant to be t_{sed}.

Now, dividing by dt and holding r constant we have

$$\left(\frac{\partial c}{\partial t}\right)_r = \left(\frac{\partial c}{\partial t}\right)_{s^*} + \left(\frac{\partial c}{\partial s^*}\right)_t \left(\frac{\partial s^*}{\partial t}\right)_r \tag{2}$$

and after a brisk rearrangement, we have an exact expression for the unnormalized, apparent sedimentation coefficient distribution function:

$$\left(\frac{\partial c}{\partial s^*}\right)_t = \left[\left(\frac{\partial c}{\partial t}\right)_r - \left(\frac{\partial c}{\partial t}\right)_{s^*}\right]\left[\left(\frac{\partial t}{\partial s^*}\right)_r\right] \equiv \hat{g}(s^*) \tag{3}$$

Its computation would require computing both the time derivative of the concentration at constant r as well as the time derivative at constant s^* at each point in the boundary. Computation of the time derivative at constant r results in complete elimination of the time-independent baseline, which is purely a function of r, as we have seen before[6]; however, computation of the time derivative at constant s^* does not remove the baseline contribution. In fact, it can be shown that Eq. (3) is analytically identical to the equation of Bridgman[34] and, therefore, must contain all the baseline components. For comparison, an unnormalized relation of the Bridgman form can be derived simply by considering c as a function of r and t, $c = c\,(r, t)$:

$$dc = \left(\frac{\partial c}{\partial r}\right)_t dr + \left(\frac{\partial c}{\partial t}\right)_r dt$$

and then, dividing through by ds^* and holding t constant, we have

$$\hat{g}(s^*) \equiv \left(\frac{\partial c}{\partial s^*}\right)_t = \left(\frac{\partial c}{\partial r}\right)_t \left(\frac{\partial r}{\partial s^*}\right)_t$$

For sufficiently high molecular weight species it follows that

$$\left(\frac{\partial c}{\partial t}\right)_{s^*} \cong \left(\frac{\partial c}{\partial t}\right)_p = -2\omega^2 \int_{s^*=0}^{s^*=s^*} s^* \left(\frac{\partial c}{\partial s^*}\right)_t ds^* \tag{4}$$

because

$$\lim_{D\to 0}\left(\frac{\partial c}{\partial t}\right)_{s^*} = \lim_{M\to\infty}\left(\frac{\partial c}{\partial t}\right)_{s^*} = \left(\frac{\partial c}{\partial t}\right)_p \quad \text{for } s > s^* \tag{5}$$

and

$$\lim_{D\to 0}\left(\frac{\partial c}{\partial t}\right)_{s^*} = \lim_{M\to\infty}\left(\frac{\partial c}{\partial t}\right)_{s^*} = 0 \quad \text{for } s < s^* \tag{6}$$

where s is the sedimentation coefficient of the component under consideration; and the subscript p is meant to designate the plateau region, the region centrifugal to the boundary.

This approximation leads to the equation derived previously for the apparent sedimentation coefficient computed from the time derivative for the special case of $D = 0$.[6]

$$\hat{g}(s^*)_t = \left(\frac{\partial c}{\partial s^*}\right)_t = \left[\left(\frac{\partial c}{\partial t}\right)_r + 2\omega^2 \int_{s=0}^{s=s^*} s^* \left(\frac{\partial c}{\partial s^*}\right)_t ds^*\right]\left[\left(\frac{\partial t}{\partial s^*}\right)_r\right] \quad (7)$$

giving validity to the use of this relation, for higher molecular weight molecules, even when diffusion is present.

For low molecular weight components (molar mass less than about 30 kg/mol at 60,000 rpm), diffusion can lead to small but significant systematic errors in the shape of $g(s^*)$ patterns computed using Eq. (7). See below for further discussion.

Simulations

Simulations of sedimentation patterns shown here were carried out on a Digital Equipment Corporation (Beaverton, OR) Alpha Server 1000 4/233 computer using the finite element method of Claverie *et al.*[36,37] with FORTRAN code executing the basic algorithm kindly supplied by D. J. Cox. The original algorithm was modified as described below to include the mass action calculations at each step of simulation for the rapidly reversible cases and to include the kinetic relaxation calculations at each step for the kinetically controlled systems according to Cox and Dale.[5] Calculations were carried out in a 1600-point grid from meniscus to base with a 1-sec time interval between iterations. After each step of sedimentation and diffusion, the concentrations of all species were recomputed either according to the law of mass action or according to the kinetic equations describing the system.

Two types of rapidly reversible associating systems were treated: a self-associating system and a heterologous interacting system. The self-associating system (a monomer–dimer–tetramer–octamer system meant to simulate myosin minifilament formation) was treated as a single concentration-dependent component whose sedimentation coefficient was taken as the weight average value at each position-dependent concentration value. The diffusion coefficient was taken as the gradient average value at each point in the cell. After each step of sedimentation and diffusion, the concentration of each species at each point along with s_w was interpolated from a look-up table computed once at the beginning of the simulation. The

[36] J.-M. Claverie, H. Dreux, and R. Cohen, *Biopolymers* **14,** 1685 (1975).
[37] J. M. Claverie, *Biopolymers* **15,** 843 (1976).

following relationships were used to treat the reequilibration after each step for the rapidly reversible system as well as for the initial equilibrium condition for the kinetically limited system.

$$2A_1 = A_2 \qquad c_2 = K_2 c_1^2 \tag{8}$$
$$2A_2 = A_4 \qquad c_4 = K_4 c_2^2 \tag{9}$$
$$2A_4 = A_8 \qquad c_8 = K_2 c_4^2 \tag{10}$$

Conservation of mass requires that the total mass concentration, C_{tot}, be given by

$$C_{tot} = c_1 + c_2 + c_4 + c_8 \tag{11}$$

where c_i is the concentration of species A_i on the c-scale.

The weight average sedimentation coefficient at each point was computed as

$$s_w = \{c_1 s_1 + c_2 s_2 + c_4 s_4 + c_8 s_8\}/C_{tot} \tag{12}$$

The gradient average value of the diffusion coefficient was computed as follows:

$$D_{ave} = \{(\partial c_1/\partial r)_t D_1 + (\partial c_2/\partial r)_t D_2 + (\partial c_4/\partial r)_t D_4 + (\partial c_8/\partial r)_t D_8\}/(\partial C_{tot}/\partial r)_t \tag{13}$$

and D_i is the diffusion coefficient of species i ($i = 1, 2, 4, 8$). As explained by Cox and Dale,[5] it is necessary to use the gradient average diffusion coefficient instead of the more common Steiner relation[38] for the average value of D if one is considering position-dependent (i.e., pressure-dependent) equilibrium constants.

For the kinetically limited cases, the rate equations were expanded to first order in the differential of time. The kinetically limited monomer–dimer–tetramer–octamer system was represented by the following three chemical equations and their corresponding linearized rate equations:

$$2A_1 \underset{k_{2,r}}{\overset{k_{2,f}}{\rightleftharpoons}} A_2 \qquad 2A_2 \underset{k_{4,r}}{\overset{k_{4,f}}{\rightleftharpoons}} A_4 \qquad 2A_4 \underset{k_{8,r}}{\overset{k_{8,f}}{\rightleftharpoons}} A_8 \tag{14}$$

$$\Delta c_1 = [k_{2,r} c_2 - k_{2,f} c_1^2]\Delta t \tag{15}$$
$$\Delta c_2 = [k_{2,f} c_1^2 + k_{4,r} c_4 - k_{4,f} c_2^2 - k_{2,r} c_2]\Delta t \tag{16}$$
$$\Delta c_4 = [k_{4,f} c_2^2 + k_{8,r} c_8 - k_{8,f} c_4^2 - k_{4,r} c_4]\Delta t \tag{17}$$
$$\Delta c_8 = [k_{8,f} c_4^2 - k_{8,r} c_8]\Delta t \tag{18}$$

[38] R. F. Steiner, *Arch. Biochem. Biophys.* **49,** 400 (1954).

The value of Δt was adjusted at each radial position so that each relaxation step was carried out with a value of Δc_i that was no more than $0.01c_i$. The concentration changed rapidly at some points, especially near the meniscus and base at the beginning of the run, requiring subdividing each 1-sec transport time step into as many as 1000 kinetic relaxation steps before proceeding to the next step of transport. For most of the more slowly varying cases ($k_r < 10^{-3}$ sec^{-1}), only 10 steps were required.

The rapidly reversible heterologous interacting system (meant to simulate an antigen–antibody reaction) was treated as follows[9]:

$$A + B = C \tag{19}$$
$$C + B = D \tag{20}$$

where A in this example represents a single-chain dimeric antibody molecule having 2 binding sites; B represents the antigen; C represents the singly liganded complex; and D represents the doubly liganded complex.

Sedimentation patterns were simulated for various molar ratios for total A and B and for various values of the equilibrium constants defined by the following equations:

$$K_1 = \frac{[C]}{[A][B]} \tag{21}$$

$$K_2 = \frac{[D]}{[C][B]} \tag{22}$$

where square brackets indicate the molar concentration of each species.

Conservation of mass requires that

$$[A]_0 = [A] + [C] + [D] \tag{23}$$
$$[B]_0 = [B] + [C] + 2[D] \tag{24}$$

Substituting and rearranging, we arrive at

$$[A] = [A]_0/\{1 + K_1[B] + K_1K_2[B]^2\} \tag{25}$$
$$[B] = [B]_0/\{1 + K_1[A] + 2K_1K_2[A][B]\} \tag{26}$$
$$[C] = K_1[A][B] \tag{27}$$
$$[D] = K_1K_2[A][B]^2 \tag{28}$$

The values of [A] and [B] were computed from Eqs. (25) and (26), using a simple iterative routine starting with an initial guess for [B]. The values of [C] and [D] were computed from the values of [A] and [B] with Eqs. (27) and (28).

The total mass concentration, C_t, is given by

$$C_t = c_A + c_B + c_C + c_D \tag{29}$$

where $c_X = [X]M_X$, X = A, B, C, or D, and M_X is molar mass of species X.

The weight average sedimentation coefficient at any point is given by

$$s_w = \{c_A s_a + c_B s_b + c_C s_c + c_D s_d\}/C_t \tag{30}$$

The value of s_w is a unique function of the total macromolecular concentration for a given ratio of total A to total B and values of K_1 and K_2. In the analysis of the data presented below, the equilibrium constants were assigned values such that the intrinsic binding constant, K_{int}, was the same for all steps, requiring that $K_1 = 4K_2 = 2K_{int}$. This was meant to simulated simple binding with no cooperativity.

Pressure dependence for this system was treated by allowing the intrinsic equilibrium constant to vary with radial position according to

$$K_{int}(r) = K_{int}(r_m) \exp\left(-\frac{\omega^2(r^2 - r_m^2)\rho\Delta V}{2RT}\right) \tag{31}$$

where $K_{int}(r)$ is the value of K_{int} at radial position r, $K_{int}(r_m)$ is the value of K_{int} at the meniscus ($P \approx 1$ atm), ρ is the solution density, ΔV is the molar volume change in cubic centimeters per mole of complex, R is the gas constant, and T is the absolute temperature.[8,9]

The rate equations for kinetically limited heterologous interactions were treated in terms of the following model, involving two binding sites for B on A,

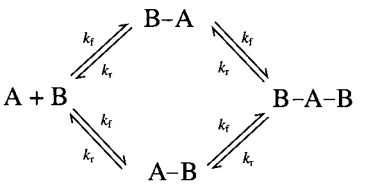

in which k_f/k_r is equal to K_{int}, the intrinsic molar equilibrium constant, and is assumed to be the same for all steps. This system can be represented by the following set of linearized rate equations:

$$\Delta C_A = [-2k_f C_A C_B + k_r C_C]\Delta t \tag{32}$$
$$\Delta C_B = [-2k_r C_A C_B + k_r C_C - k_f C_B C_C + 2k_r C_D]\Delta t \tag{33}$$
$$\Delta C_C = [2k_f C_A C_B - k_r C_C - k_f C_B C_C + 2k_r C_D]\Delta t \tag{34}$$
$$\Delta C_D = [k_f C_B C_C - 2k_r C_D]\Delta t \tag{35}$$

where C_A, C_B, C_C, and C_D are molar concentrations of species A, B, C, and D, respectively; and $C_C = C_{AB} + C_{BA}$.

The relationships between the intrinsic rate constants, k_i, and the macroscopic equilibrium constants, K_i, are given by

$$K_1 = \frac{2k_f}{k_r} = 2K_{int} \quad \text{and} \quad K_2 = \frac{k_f}{2k_r} = 0.5K_{int} \tag{36}$$

In simulations, the rate constants were chosen so that $K_1 = 2K_{int}$ and $K_2 = 0.5K_{int}$ with $K_{int} = 1 \times 10^7\, M^{-1}$, $[A]_0 = 1 \times 10^{-7}\, M$, and $[B]_0 = 2[A]_0$, where K_1 and K_2 are the macroscopic equilibrium constants. The values of $[B]_0 = 2[A]_0$ correspond to the experimental situation to be presented below (Fig. 3). These kinetic equations were tested by showing that for values of $k_r > 10^{-2}$ sec^{-1}, the sedimentation profiles for all species were essentially the same as for those computed from the mass action equations above. It was also demonstrated that for values of $k_r < 10^{-9}$ sec^{-1}, the profiles corresponded to the summation of the same independently sedimenting species.

Kinetically Limited Interacting Systems and s_w

The weight average sedimentation coefficient is a composition-dependent parameter, and therefore, for an interacting system, its dependence on total protein concentration can be analyzed to determine association constants and stoichiometries. To answer the question of what effect a kinetically limited reequilibration would have on the computation of s_w, a series of sedimentation runs were simulated for various values of forward and reverse rate constants corresponding to a given value of the equilibrium constant. We consider two systems, the antigen–antibody system mentioned above and a monomer–dimer–tetramer–octamer self-associating system for which the stepwise molar equilibrium constants are equal. The equilibrium constants and initial condition were chosen so that there were equal amounts of all species present at the start of the run. The rate constants for the self-associating system were varied effectively from zero to infinity with all the forward rate constants made equal to each other and all the reverse rate constants made equal to each other for all steps.

The heterologous interacting (i.e., the antigen–antibody) system was also simulated for various values of the rate constants corresponding to a given value of the intrinsic equilibrium constant. The system was simulated as described above for $K_{int} = 1 \times 10^7\, M^{-1}$ so that $K_1 = 2K_{int}$ and $K_2 =$

$0.5K_{int}$ and $[B]_0 = 2[A]_0$ with $[A]_0 = 1 \times 10^{-7} M$. The value of s_w for each simulated curve was computed using the following relationship:

$$s_w = \frac{\int_{s^*=0}^{s^*=s_p^*} s^* g(s^*) ds^*}{\int_{s^*=0}^{s^*=s_p^*} g(s^*) ds^*}$$

where s_p^* is a value of s^* in the plateau region at which $g(s^*) = 0$[9].

For computational purposes this relation can be recast in the following discrete form:

$$s_w = \frac{\sum_{i=i}^{i=n} s_i^* g(s_i^*)}{\sum_{i=1}^{i=n} g(s_i^*)}$$

where n corresponds to a point in the plateau region where $g(s^*) = 0$.

Effect of Diffusion on Distribution Patterns

As mentioned above, for low molecular weight components (molar mass less than about 30 kg/mol at 60,000 rpm), diffusion can lead to small but significant systematic errors in the shape of $g(s^*)$ patterns computed using Eq. (7). This error, which results from the approximation used in going from Eq. (3) to Eq. (7), can cause a shift in the peak position of $g(s^*)$ from the correct value of s toward smaller values. To determine the magnitude of the factors contributing to this error, a series of simulations were carried out over a range of M and s values. The simulations showed that for a single species, the peak position of the $g(s^*)$ versus s^* curve slightly underestimates the true value of s by an amount that is dependent on the molecular weight and square of the speed but independent of the value of the sedimentation coefficient. This error is greatest at the beginning of the run and approaches zero in the limit of infinite time. For a boundary whose midpoint is located near the middle of the cell, the correction factors are given in Table I. These correction factors should be applied if accurate shape information is to be obtained from the s^* values obtained from the peak position. However, in most situations the correction is mainly an esthetic refinement to the observed patterns, the primary interest being in the general characteristics of the boundary shape and how they change under various conditions of self-association, complex formation, or ligand binding.

TABLE I
CORRECTION FACTORS FOR PEAK VALUE OF s^* IN $g(s^*)$ PLOTS AS FUNCTION OF MOLECULAR WEIGHT AND SPEED[a]

s^*_{peak}/s_{true}	M (kg/mol)[b]	Speed (rpm)[c]	$(M \cdot rpm^2) \times 10^{-12}$
0.99	60.0	60,000	216
0.98	35.0	46,000	129
0.97	25.0	39,000	90
0.96	18.0	33,000	65

[a] These factors become important and should be taken into account if accurate shape information is to be obtained from s^*_{peak}. The factors s^*_{peak} and s_{true} are dependent on the product $M\omega^2$.
[b] Assuming $r_m = 5.9$ and $r_{mid} = 6.5$ cm. At 60,000 rpm.
[c] Assuming $r_m = 5.9$ and $r_{mid} = 6.5$ cm. M = 60.0 kg/mol, where r_m is the meniscus, r_{mid} is the radius of the midpoint of the boundary, and M is molar mass.

Antigen–Antibody System

The interaction between a single-chain antibody construct, 741F8 $(sFv')_2$, and the extracellular domain (ECD) of the c-*erbB*-2 oncogene product was studied in the 0.1 to 10 μM range to determine the equilibrium constant for the interaction. This system had been partially characterized at higher concentrations.[39,40] Data from those earlier studies are plotted in Figs. 1[31,32,39,41] and 2. The 741F8 $(sFv')_2$ sedimented at $s_{20,w} = 3.4S$ and the ECD, at $s_{20,w} = 4.3S$, while the 1:1 mixture behaved as a reaction boundary with a peak position at about 7.0S. When excess ECD was added to drive the reaction toward completion, the value of s^* corresponding to the peak in the reaction boundary moved to about 7.9S (Fig. 2). From this observation, a value of 8.0S was taken as the value for the doubly liganded complex for the purposes of simulation and curve fitting. Under these conditions (2–4 μM) the 2:1 complex is predominantly populated.

To observe the dissociation process and to obtain data to be used for the estimation of the equilibrium constants, the 1:2 mixture was run in the range of 0.03 to 0.3 μM, where significant disssociation could be observed.

[39] G. P. Adams, J. E. McCartney, M. S. Tai, H. Oppermann, J. S. Huston, W. F. Stafford, M. A. Bookman, I. Fand, L. L. Houston, and L. M. Weiner, *Cancer Res.* **53,** 4026 (1993).
[40] J. E. McCartney, M. S. Tai, R. M. Hudziak, G. P. Adams, L. M. Weiner, D. Jin, W. F. Stafford, S. Liu, M. A. Bookman, A. A. Laminet, I. Fand, L. L. Houston, H. Oppermann, and J. S. Huston, *Protein Eng.* **8,** 301 (1995).
[41] S. Liu and W. F. Stafford, *Anal. Biochem.* **224,** 199 (1995).

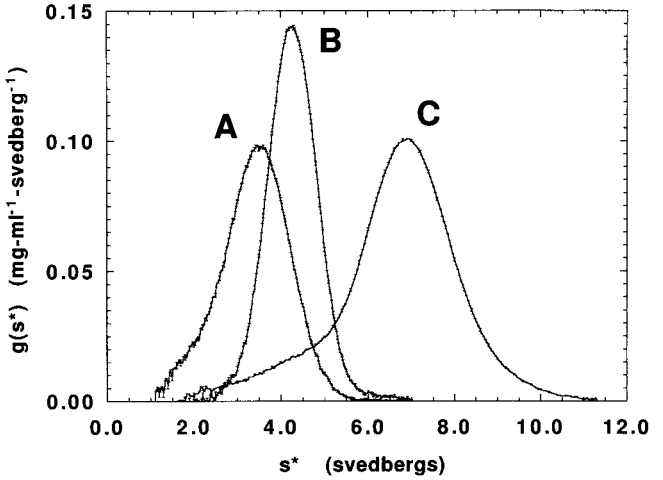

FIG. 1. Demonstration of a heterologous interaction between a single-chain antibody and its antigen. (A) 741F8 $(sFv')_2$ (4.5 μM)(t_{sed} = 6547 sec); (B) ECD (3.4 μM); (C) mixture of 741F8 $(sFv')_2$ (1.89 μM)(t_{sed} = 6552 sec) and ECD (3.4 μM)(t_{sed} = 4132 sec). Recombinant extracellular domain (ECD) of the c-ErbB-2 oncoprotein and recombinant dimeric single-chain antibody 741F8 $(sFv')_2$ were prepared as described previously.[39] The experiments were carried out in an AN-F Ti rotor on a Beckman Instruments model E equipped with on-line Rayleigh optics as described previously,[31] using either three or four 12-mm cells and run at 56,000 rpm at 20°. Experiments were also carried out on a Beckman Optima XL-A equipped with on-line Rayleigh optics as described previously,[32] using four cells in an AN-60 titanium rotor at 20°. Temperature calibration was carried out with ethanolic cobalt chloride solutions as an optical thermometer.[41]

The samples were run at nominal loading concentrations of $[(sFv')_2] = 3.0 \times 10^{-7}, 1.0 \times 10^{-7}, 0.3 \times 10^{-7} M$ corresponding to total protein concentrations of 70, 23, and 8 μg/ml, respectively. Figure 3 shows the experimental curves obtained from this dilution series. Along with the experimental curves are plotted the simulated curves generated for a value of $1.0 \times 10^7\ M^{-1}$ for K_{int} and the actual loading concentrations. The experimental loading concentrations were estimated by integrating the $g(s^*)$ curves to get the plateau concentration and then corrected to the initial concentration taking radial dilution into account. These values of the initial concentrations were then used as input parameters for the simulated curves. There is some deviation at higher s^* values at the highest loading concentration, suggesting possible further aggregation, possibly self-association of the complex. Molecular weights higher than that expected for the 1:2 complex were also seen in sedimentation equilibrium runs at higher concentrations (W. F. Stafford, unpublished observations, 1994). The value of $K_{int} = 1 \times 10^7\ M^{-1}$ agrees well with the value of $K_{eq} \sim 2 \times 10^7\ M^{-1}$ obtained by surface plasmon resonance.[39]

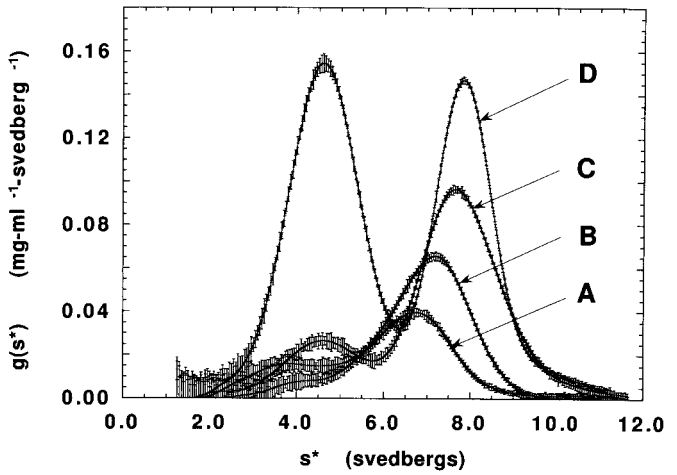

FIG. 2. Demonstration of equilibrium binding of ECD by 741F8 $(sFv')_2$. The two components were mixed in various ratios to determine the stoichiometry of binding (A) 0.5 mol of ECD/mol of $(sFv')_2$, (B) 1.0 mol of ECD/mol of $(sFv')_2$ (C) 2.0 mol of ECD/mol of $(sFv')_2$ and (D) 4.0 mol of ECD/mol of $(sFv')_2$. The 1 : 1 complex is expected to have a sedimentation coefficient of about 5.9–6.0S based on the interaction of an anti-c-ErbB-2 Fab (3.5S) with the ECD (data not shown here).

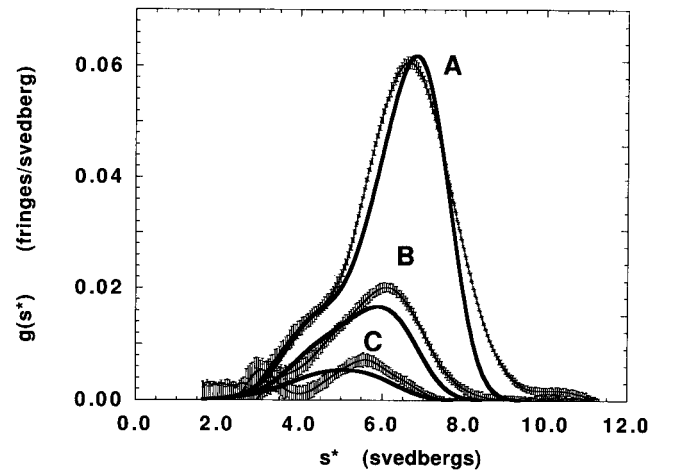

FIG. 3. Dilution series of ECD by 741F8 $(sFv')_2$ at stoichiometric ratio of [ECD]/[$(sFv')_2$] = 2.0. The 741F8 $(sFv')_2$ (molecular mass of 52 kDa) was combined with 2 mol of the ECD (90 kDa) so that $[ECD]_0 = 2[(sFv')_2]_0$. The solid curves are simulated data using $K_{int} = 1 \times 10^7 M^{-1}$, using values of $[(sFv')_2]_0$ corresponding to the values loaded into the cell, which were determined by integrating the $g(s^*)$ curves, corrected for radial dilution, to obtain $c_0 = \int g(s^*)ds^*$. Several guesses for K_{int} spanning 0.5×10^{-7} to $2.0 \times 10^{-7} M^{-1}$ were tried. Visual comparison with the data led to the choice shown.

Effect of Kinetically Limited Reequilibration on Computation of s_w

To address the question of the effect that kinetically limited reequilibration would have on the computation of equilibrium constants from the analysis of weight average sedimentation coefficients, extensive simulations were carried out for a range of forward and reverse rate constants. It was found that kinetically limited reequilibration during sedimentation would not significantly affect the computation of reliable values of s_w for an interacting system as long as the system was at equilibrium at the start of the run. The simulations shown in Fig. 4 for the monomer–dimer–tetramer–octamer system gave the same value of s_w to within the usual experimental error over the entire range of rate constants from infinitely fast to 10^{-9} sec^{-1} for the first-order dissociation rate constants for the same value of $K_{int} = 1 \times 10^7\ M^{-1}$. The systems were simulated for values of the equilibrium constant selected such that the systems were poised at the most concentration-sensitive conditions with nearly equal amounts of all species present at the start of the run. Parameters estimated from these systems show little sensitivity to radial dilution.

The systems were compared at the same sedimentation time for different values of the rate constants as well as at different times for the same value of the rate constants. The weight average sedimentation coefficient computed for either the self- or heteroassociating system was independent

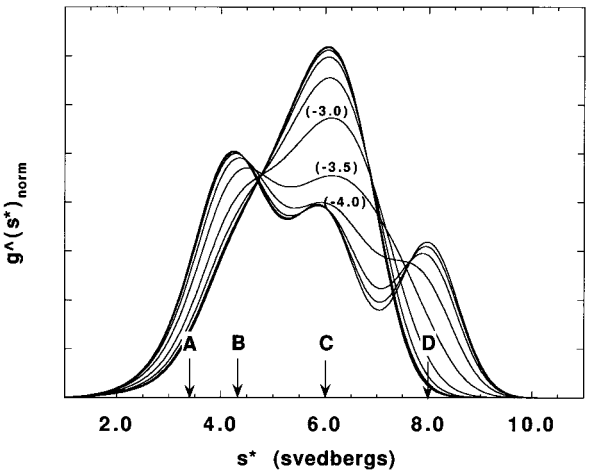

FIG. 4. Effect of different rates of reequilibration on the time derivative patterns and on the computation of s_w for a simulated antigen–antibody system corresponding to the sFv–ECD system described in Figs. 1–3. A, B, C, and D indicate the sedimentation coefficients of the species in equilibrium: 3.4, 4.3, 6.0, and 8.0S, respectively. See text for description of the kinetic model and other details of the reactions.

of either time or the rate constants, with a variation of only about 3% over the entire range of time and rate constant values. One might expect a decrease in weight average sedimentation coefficient as a function of time for two reasons: First, for a noninteracting system, s_w decreases with time because the faster moving components will have experienced greater radial dilution at any given time than the more slowly moving ones. Therefore, the plateau composition will change with time because the more rapidly sedimenting species will be removed more rapidly from the system than the more slowly sedimenting species. Second, for a rapidly reversible, interacting system, the weight average sedimentation coefficient will decrease because of the shift of the equilibrium by mass action as the plateau concentration decreases.

However, it can be shown that neither one of these effects results in serious error in the estimation of s_w. Sedimentation patterns were generated for various values of the rate constants for the heterologous system, both as a function of time and for various values of the reverse rate constant, k_r, for the values of the parameters shown in Fig. 4. Similar analysis was carried out for the monomer–dimer–tetramer–octamer system (Fig. 5). Figure 6 shows time series for a wide range of values of k_f and k_r (10^{-9} sec$^{-1} < k_r < \infty$) corresponding to the given equilibrium constants.

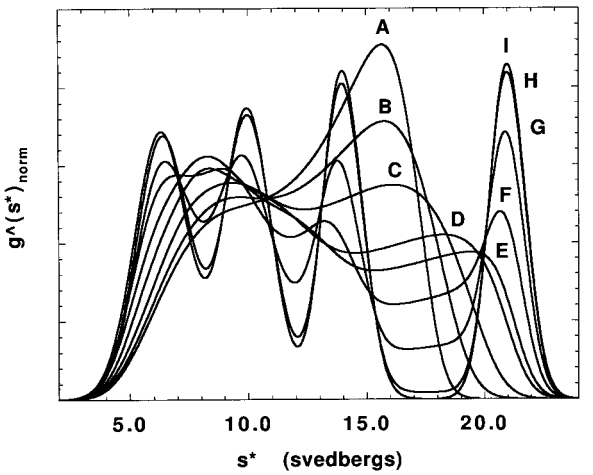

FIG. 5. Effect of different rates of reequilibration on the time derivative patterns and on the computation of s_w for a simulated monomer–dimer–tetramer–octamer system. Curves A through H correspond to values of k_r of infinite, 10^{-2}, 3×10^{-3}, 10^{-3}, 7×10^{-4}, 3×10^{-4}, 10^{-4}, 10^{-5}, and 10^{-9} sec^{-1}, respectively. (s_1 = 6.4S, D_1 = 1.26F, s_2 = 10.0S, s_3 = 14.0S, and s_4 = 21.0S); C_{tot} = 4 g/liter, $k_f/k_r = K_{12} = K_{24} = K_{48}$ = 1.0 liter/g.) See text for further details and Table II for values of s_w computed from these curves. The values chosen here for K and C_{tot} forces the weight fraction of each species to be 0.25 at the start of the run.

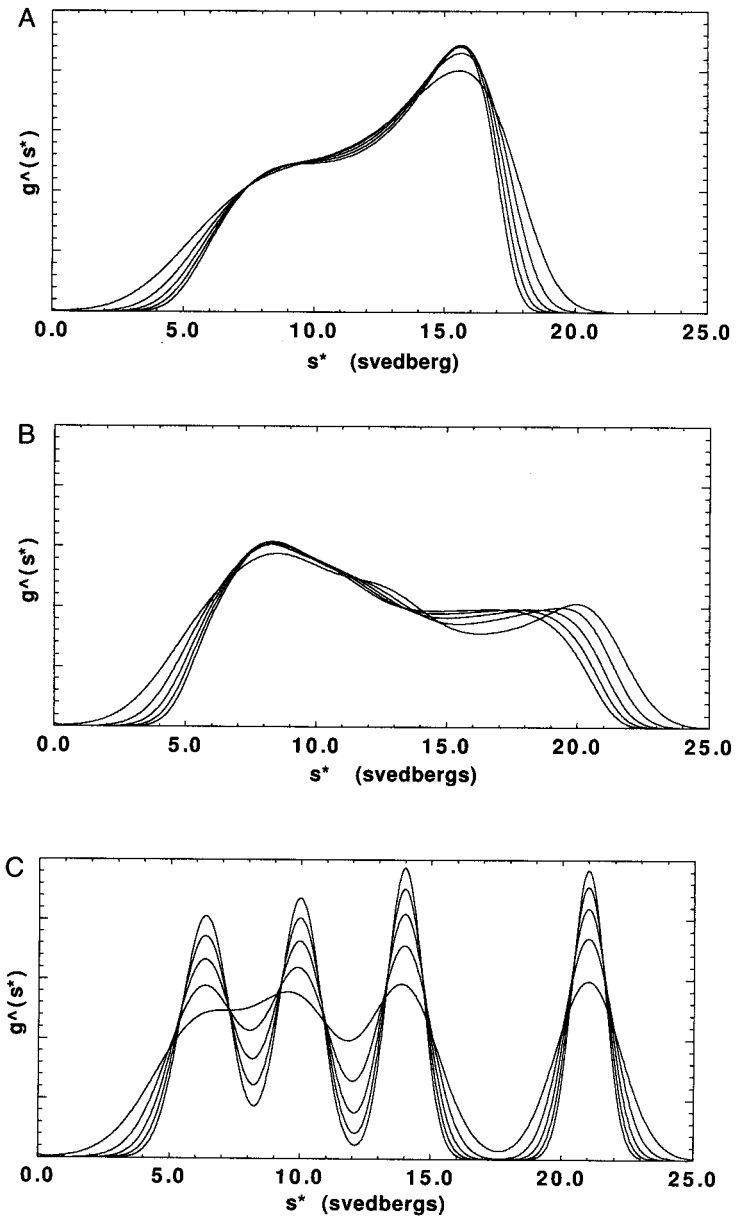

FIG. 6. Effects of radial dilution on computation of s_w for the monomer–dimer–tetramer–octamer system at various rates of reequilibration; the system is the same as that shown in Fig. 5: Time series for (A) $k_f = \infty$, $k_r = \infty$; (B) $k_f = 10^3$/liters-g^{-1} sec^{-1}, $k_r = 10^{-3}$ sec^{-1}; and (C) $k_f = 10^{-9}$ liter g^{-1} sec^{-1}, $k_r = 10^{-9}$ sec^{-1}. Times of sedimentation were 1440, 2400, 3360, 4320, and 5280 sec, respectively. (*Note:* Narrower curves are from later times.)

TABLE II
s_w COMPUTED AFTER VARIOUS TIMES OF SEDIMENTATION FOR MONOMER–DIMER–TETRAMER–OCTAMER SYSTEM[a]

t_{sed} (sec)	$s_{w,true}$[b] ($k_f = k_r = \infty$)	s_w, computed: $k_f = \infty$, $k_r = \infty$	$k_f = 10^{-3}$[c], $k_r = 10^{-3}$	$k_f = 10^{-4}$, $k_r = 10^{-4}$	$k_f = 10^{-9}$, $k_r = 10^{-9}$	$s_{w,true}$[d] ($k_f = k_r = 0$)
1440	12.67S	12.23	12.45	12.56	12.59	12.74
2400	12.55	12.41	12.50	12.54	12.59	12.67
3360	12.43	12.39	12.31	12.48	12.54	12.60
4320	12.32	12.35	12.28	12.41	12.48	12.53
5280	12.20	12.30	12.21	12.33	12.42	12.46

[a] As described in text.
[b] The value of $s_{w,true}$ was computed from the law of mass action at the plateau concentration and represents the instantaneous "true" value of s_w as opposed to the "cumulative average," which is the value computed from the $g(s^*)$ versus s^* curves.
[c] Units of k_f are liters g^{-1} sec^{-1} and the units of k_r are sec^{-1}. The values of k_f and k_r are the same for all steps so that $K_{eq} = 1.0$ liter/g and $C_0 = 4.0$ g/liter. This forces the weight fraction of all four species to be 0.25 at the start of sedimentation.
[d] Computed from radial dilution relation, $c_p/c_0 = \exp(-2\omega^2 st)$, for each component in the mixture. It corresponds to the instantaneous "true" value of s_w as described above. The value of s_w corresponding to the initial loading concentration is 12.85S and is the same for all cases. The values of s and D for the individual species are $s_1 = 6.4$S, $D_1 = 1.26$F, $s_2 = 10.0$S, $s_4 = 14.0$S, $s_8 = 21.0$S (speed, 34,000 rpm).
Note: The maximum variation of s_w over the entire range shown is 4%.

The most interesting result of these simulations is that the value of s_w is essentially independent of the values of the rate constants for particular values of the equilibrium constants as long as the system is at equilibrium at the start of the run. Moreover, they show that, because the values of s_w are essentially independent of time, radial dilution has only an insignificant effect on the estimation of s_w. Table II summarizes the results of four simulations for various rates of reequilibration of the monomer–dimer–tetramer–octamer system. In each case the system was initially at equilibrium. The heterologous system represents a less extreme case than the monomer–dimer–tetramer–octamer system and was found to be even less sensitive to radial dilution.

Effects of Radial Dilution on Computation of s_w

Radial dilution arises because of the sectorial shape of the centrifuge cell. As material sediments, it is transported into regions of larger cross-sectional area and, therefore, larger volume. The dilution it experiences is

proportional to the square of the distance traveled from the center of rotation. The plateau concentration decreases about 21% as the boundary position moves from 5.9 to 6.5 cm. This dilution will cause a shift in the equilibrium concentrations of sedimenting species, leading to a decrease in s_w with time. It can be shown, in spite of radial dilution, that for many systems the effects of radial dilution on the computation of s_w do not introduce serious errors into the determination of equilibrium constants computed from s_w. For the case of the simulated monomer–dimer–tetramer–octamer system (Figs. 5 and 6), the effects of radial dilution on s_w were seen to be insignificant (Table II) over a wide range in sedimentation time after the boundary had cleared the meniscus.

Pressure-Dependent, Reversible Interactions

Negative concentration gradients produced by pressure-dependent, reversibly interacting systems can be sustained only in the presence of a stabilizing gradient of an additional component. Density gradients established by redistribution of buffer components during sedimentation are often sufficient to stabilize moderate negative concentration gradients. To demonstrate this source of stabilization, the density gradient set up by the redistribution of 0.1 *M* NaCl at 56,000 rpm was simulated using $\bar{v}_3 = 0.33$ cm^3/g, $s = 0.24$S, and $D = 150 \times 10^{-7}$ cm$^2 \cdot$ sec^{-1}. The density distribution set up by the macromolecular system was added to the density distribution of NaCl to compute the total density gradient from the following relationship: $\rho(r) = \rho_0 + (1 - \bar{v}_2\rho_0)c_2 + (1 - \bar{v}_3\rho_0)c_3$, where c_i $(i = 2, 3)$ is the concentration in units of g/cm^3 of protein and NaCl, respectively, as a function of position, and $\rho_0 = 0.9982$ at 20°.

The macromolecular system used for the simulation of pressure effects was the antigen–antibody system described above but with a volume change of +1000 cm^3/mol on association for each step (Fig. 7).[9] If the simulation

FIG. 7. Stabilization of pressure effects. Salt and buffer redistribution can stabilize negative macromolecular concentration gradients. (A) The apparent sedimentation coefficient distribution function for the system A + 2B = D for various values of ΔV at $\theta = [A]_0 K_{int} = 1.0$. (a) $\Delta V = 10{,}000$ (b) $\Delta V = 1000$, (c) $\Delta V = 0$ cm^3/mol. (B) Simulation of salt redistribution to stabilize negative concentration gradients generated by pressure-dependent complex formation with a volume change of association of +1000 cm^3/mol. (a) Density distribution of 0.1 *M* NaCl after 1800 sec of sedimentation with instantaneous acceleration, (b) total density distribution, (c) protein concentration distribution. (C) Comparison of plots of total density distributions reached after an equivalent sedimentation time of 600 sec at 56,000 rpm (i.e., same value of $\int \omega^2 dt = 2.06 \times 10^{10}$ sec^{-1}). Final speed, 56,000 rpm, with (a) instantaneous acceleration to final speed, (b) acceleration at 5000 rpm/min, and (c) acceleration at 2000 rpm/min.

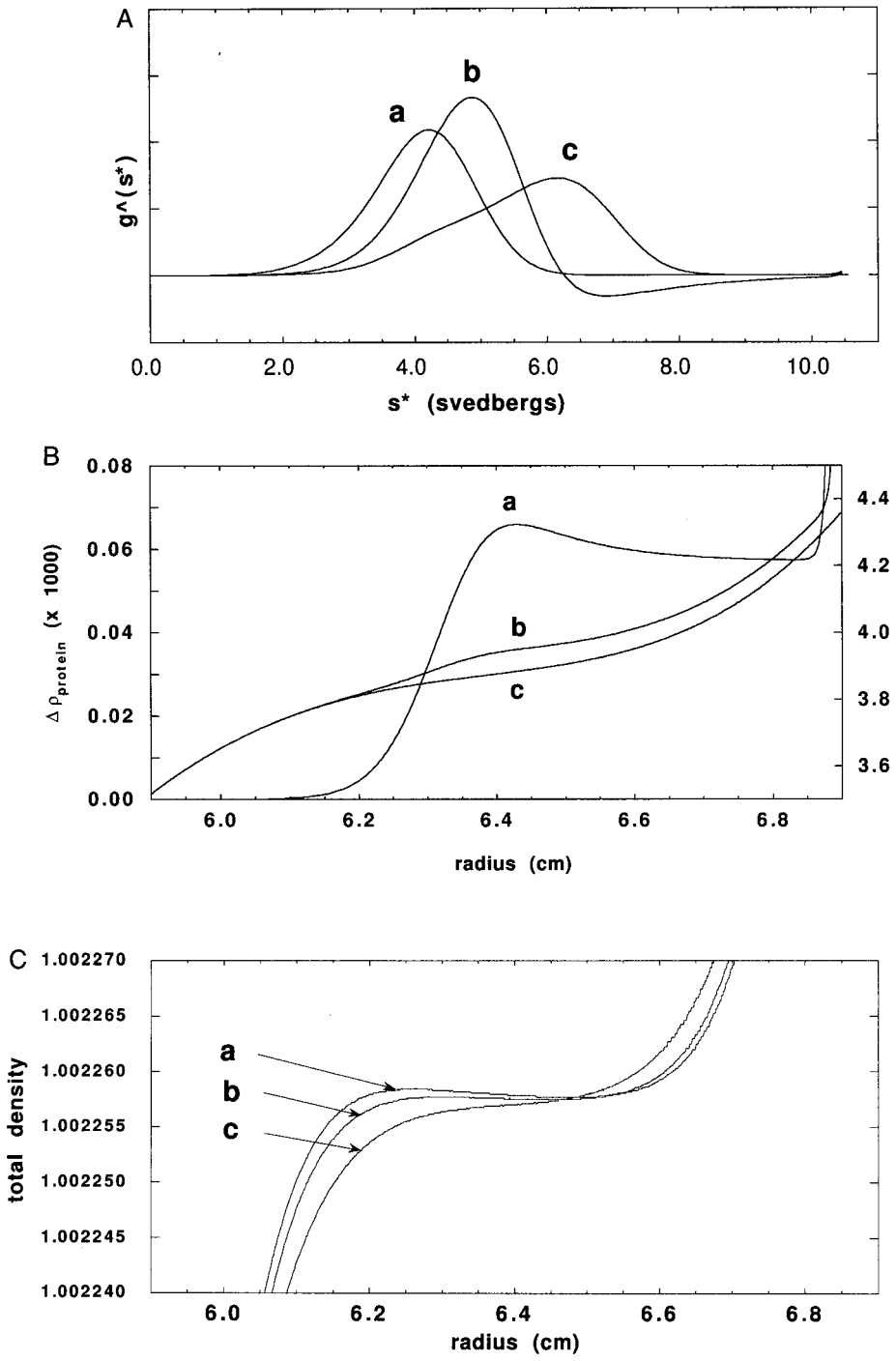
A
a
b
c
g^(s*)
0.0
2.0
4.0
6.0
8.0
10.0
s* (svedbergs)
B
a
b
c
0.08
0.06
0.04
0.02
0.00
Δ ρprotein (x 1000)
4.4
4.2
4.0
3.8
3.6
Δ ρ x (1000)
6.0
6.2
6.4
6.6
6.8
radius (cm)
C
a
b
c
1.002270
1.002265
1.002260
1.002255
1.002250
1.002245
1.002240
total density
6.0
6.2
6.4
6.6
6.8
radius (cm)

was allowed to start instantaneously at full speed (56,000 rpm), it was found that a negative gradient was set up initially and dissipated after about 15 min of sedimentation time as the NaCl redistributed. If, however, acceleration was allowed to take place at the rate of 5000 rpm/min, no overall negative gradient was established, and at the rate of 2000 rpm/min, no negative gradients were established before sufficient salt redistribution had taken place to stabilize the system.

The volume change of +1000 cm^3/mol used here is a rather extreme case for this type of system (simple complex formation); therefore, one may conclude that convection should not be a problem for most dilute interacting systems exhibiting a volume change on association as long as normal amounts of salt are present and acceleration rates are kept below 5000 rpm/min. On the other hand, for large macromolecular assemblies like myosin filaments,[42] for which the molar volume change is much larger, density gradients established during sedimentation by salt redistribution usually will not be sufficient to stabilize the system against convection.

Discussion

Methods for the analysis of interacting systems by analytical ultracentrifugation using the time derivative of the concentration profile have been discussed. The time derivative of the concentration profile can be converted into an apparent sedimentation coefficient distribution function, $g(s^*)$ versus s^*, that is geometrically similar to the gradient plots of dn/dr versus r that are produced by schlieren optics. Therefore, these patterns, which are of much higher precision than the corresponding schlieren patterns, can be used to study interacting systems at much lower concentrations than could be done previously by sedimentation velocity using refractometric optics. Typically, schlieren optics in 12-mm cells limited the range of concentration to 1 mg/ml and above. With interference optics and time derivative methods, the concentration range has been expanded to the 1- to 10-μg/ml range. An antigen–antibody system having an intrinsic equilibrium constant of $1 \times 10^7\ M^{-1}$ was studied at protein concentrations ranging from 8 to 70 μg/ml, corresponding to 1.3×10^{-8} to $3 \times 10^{-7}\ M$ complex. The equilibrium constant was obtained for this system by comparison of simulated sedimentation patterns with the observed patterns.

Weight average sedimentation coefficients can be computed from the time derivative patterns. Because weight average sedimentation coefficients are composition dependent, depending only on the plateau concentrations of the species comprising a particular system, they can be used to obtain

[42] R. Josephs and W. F. Harrington, *Biochemistry* **7**, 2834 (1968).

thermodynamic information such as stoichiometries and association equilibrium constants. Several questions concerning the effects of kinetics of reequilibration and the effect of radial dilution on the computation of s_w were considered. It was concluded that neither kinetically limited reequilibration nor radial dilution would be expected to introduce serious errors into the computation of s_w as long as the system is at equilibrium at the start of the run.

Pressure-dependent systems were also considered. It had been previously shown, in the absence of stabilizing density gradients, that the potential for convection exists for any interacting system that has a finite volume change on association. By use of simulations of buffer redistribution at typical salt concentrations, it is shown here that these negative concentration gradients can be stabilized by redistribution of buffer components under appropriate conditions, allowing the analysis of systems with moderate volume changes by sedimentation velocity.

Work is currently underway to incorporate these simulation routines into a nonlinear fitting algorithm to provide greater flexibility in treating interacting systems by time derivative methods.[23] A program called ABCDFitter is available from the author for fitting to time difference data to analyze one- or two-step complex formation. A detailed description of this algorithm and software will appear elsewhere.

Acknowledgments

I thank A. Garcia, T. Laue, and M. Jacobsen for detailed critical reading of this manuscript.